

LATTICE DYNAMICS OF EQUIATOMIC BINARY ALLOYS

ADITYA M. VORA

Parmeshwari 165, Vijaynagar Area, Hospital Road, Bhuj – Kutch, 370 001, Gujarat, India
Tel.: +91-2832-256424, E-mail address: voraam@yahoo.com

Received 3 November 2006; Revised manuscript received 1 March 2008

Accepted 3 December 2008 Online 28 January 2009

In the present article, the calculations of the lattice dynamical properties of four equiatomic binary alloys viz. $\text{Na}_{0.5}\text{Li}_{0.5}$, $\text{Na}_{0.5}\text{K}_{0.5}$, $\text{Na}_{0.5}\text{Rb}_{0.5}$ and $\text{Na}_{0.5}\text{Cs}_{0.5}$ to second order in local model potential is discussed in terms of real-space sum of Born von Karman central force constants. Well known Ashcroft's empty core (EMC) model potential has been used to study the lattice dynamical properties. Instead of the average of the force constants of metallic Li, Na, K, Rb and Cs, the pseudo-alloy-atom (PAA) is adopted to compute directly the force constants of four equiatomic sodium-based binary alloys. The exchange and correlation functions due to Hartree (H) and Ichimaru-Utsumi (IU) are used to investigate influence of screening effects. Results for the lattice constants i.e. C_{11} , C_{12} , C_{44} , $C_{12} - C_{44}$, C_{12}/C_{44} and bulk modulus (B) obtained using the Hartree screening function have higher values in comparison with the results obtained for the same properties using Ichimaru-Utsumi (IU) screening function. The results for the shear modulus (C'), deviation from Cauchy's relation (C_{12}/C_{44}), Poisson's ratio (σ), Young modulus (Y), propagation velocity of elastic waves, phonon dispersion curves and degree of anisotropy (A) are encouraging for the four equiatomic Na-based binary alloys.

PACS numbers: 63.50.+x, 62.30.+d, 62.20.-x, 62.20.Dc UDC 538.911, 539.32

Keywords: lattice dynamics, lattice dynamical properties, sodium-based equiatomic alloys

1. Introduction

In the study of various properties of solids, one frequently requires the knowledge of the interaction energy between the ions or atoms. The studies of effective interionic interactions in simple metals has a long history and originally they were not systematized and were concerned with individual metals and groups of metals. In recent years, considerable attention has been devoted to the theoretical study of

the nature of effective interaction between constituent atom or ion in simple metals [1–10].

The bcc $A_{1-x}B_x$ ($A=\text{Na}$; $B=\text{Li, K, Rb, Cs}$) binary alloy systems form substitutional solid solutions over all concentrations (x) of the second metallic component, and the crystal binding of the solid solution is unchanged compared with that of the pure alkali metals. Theoretical studies related to the lattice dynamics of the alloy systems have been devoted to $\text{Na}_{0.5}\text{Li}_{0.5}$, $\text{Na}_{0.5}\text{K}_{0.5}$, $\text{Na}_{0.5}\text{Rb}_{0.5}$ and $\text{Na}_{0.5}\text{Cs}_{0.5}$ systems. The lattice dynamics of the pure alkalis have been investigated in detail, but the work on the comprehensive study of lattice dynamical properties of their binary alloys is almost negligible in the literature [1–4]. Very recently, we have reported the lattice dynamical properties of equiatomic alkali binary alloys using model potential formalism [1–4]. Also, Gajjar et al. [5] have studied the lattice dynamics of bcc $\text{Cs}_{0.3}\text{K}_{0.7}$ alloy using model potential formalism. Only Soma et al. [7] have studied the phonon dispersion curves of $\text{Cs}_{0.7}\text{K}_{0.3}$, $\text{Cs}_{0.7}\text{Rb}_{0.3}$, $\text{Cs}_{0.3}\text{Rb}_{0.7}$ and $\text{Rb}_{0.71}\text{Cs}_{0.29}$ alloys. Experimentally, Kamitakahara and Copley [8] have studied the lattice dynamics of $\text{Rb}_{1-x}\text{K}_x$ alloys with concentration $x = 0.06, 0.18$ and 0.29 by neutron scattering technique. Recently, Chushak and Baumketner [9] have reported the dynamical properties of liquid $\text{Cs}_{0.3}\text{K}_{0.7}$ alloy. For the interatomic interaction, they have used an ancient empty-core model [9] and generated phonon dispersion curves of the liquid alloy. Hence, we have decided to study four equiatomic sodium based binary alloys i.e. $\text{Na}_{0.5}\text{Li}_{0.5}$, $\text{Na}_{0.5}\text{K}_{0.5}$, $\text{Na}_{0.5}\text{Rb}_{0.5}$ and $\text{Na}_{0.5}\text{Cs}_{0.5}$.

By treating the sodium based binary alloys as a pseudo-alloy-atom (PAA), real space sum analysis [1–5] is used to compute the radial and tangential force constants, phonon dispersion relation along three major symmetry directions, elastic constants, bulk modulus, shear modulus, Cauchy's relation, Poisson's ratio, Young modulus, propagation of elastic waves and degree of elastic anisotropy. Ashcroft's empty core (EMC) single parametric local model potential [10] is used to describe the electron-ion interaction for the pseudo-alloy-atom of sodium-based four binary alloys. For the first time, an advanced and more recent local field correlation function due to Ichimaru-Utsumi (IU) [11] has been employed the investigations. This helps in identifying the influence of exchange and correlation effects in the static form of Hartree (H) (only static) dielectric function [12].

Most of the alkalis are bcc at room temperature and Li and Na are hcp at low temperature. The present computations are performed at room temperature and also the experimental data of these alkalis are available for bcc structure only. Hence, we have adopted bcc structure throughout the computation for alkalis and their equiatomic alloys.

2. Theoretical methodology

The phonon frequencies can be obtained by solving the standard secular determinantal equation [1–6]

$$\det|D_{\alpha\beta}(q) - 4\pi^2\nu^2 M\delta_{\alpha\beta}| = 0, \quad (1)$$

where M is the ionic mass, ν is the phonon frequency and $D_{\alpha\beta}$ is the dynamical matrix in which the force between two ions depends only upon the distance between them and is given by,

$$D_{\alpha\beta}(q) = \sum_n (1 - e^{i\vec{q}\cdot\vec{r}}) \left. \frac{d^2\Phi(r)}{dr_\alpha dr_\beta} \right|_{r=\gamma_n}, \quad (2)$$

where Φ is the interionic pair potential, r_α and r_β are the α^{th} and β^{th} Cartesian components of the position vector of n^{th} ion, respectively.

This dynamical matrix element used in the present calculation finally takes the form

$$D_{\alpha\beta}(q) = \sum_n (1 - e^{i\vec{q}\cdot\vec{r}}) \left[K_t + \frac{r_\alpha r_\beta}{r^2} (K_\gamma - K_t) \right], \quad (3)$$

where K_t and K_γ are the force constants between a pair of ions interacting through a central interaction and n specifies the shell index.

$$K_t = \frac{1}{r} \frac{d\Phi(r)}{dr} = -\frac{Z^2 e^2}{r^3} + \frac{\Omega_0}{\pi^2 r^2} \int_0^\infty F(q) q^2 \left[\cos(qr) - \frac{\sin(qr)}{qr} \right] dq, \quad (4)$$

$$K_\gamma = \frac{d^2\Phi(r)}{dr^2} = \frac{2Ze^2}{r^3} + \frac{\Omega_0}{\pi^2 r^2} \int_0^\infty F(q) q^2 \left[\frac{2\sin(qr)}{qr} - 2\cos(qr) - qr \sin(qr) \right] dq. \quad (5)$$

Here $F(Q)$ is the energy wave number characteristic given by [1–4]

$$F(q) = \frac{\Omega_0 q^2}{8\pi e^2} |W_B(q)|^2 \frac{\epsilon_H(q) - 1}{1 + [\epsilon_H(q) - 1][1 - f(q)]}, \quad (6)$$

where Ω_0 , $W_B(q)$, $\epsilon_H(q)$ and $f(q)$ are the atomic volume, bare-ion pseudopotential, static Hartree dielectric function and local field correlation function, respectively.

The bare-ion pseudopotential due to Ashcroft's empty core (EMC) model potential is given by [10]

$$V(q) = -\frac{8\pi Z}{\Omega_0 q^2} \cos(qr_C), \quad (7)$$

where Z , Ω_0 and r_C are the valence, atomic volume and parameter of the model potential of four equiatomic sodium-based binary alloys, respectively.

Using these atomic-force constants, we can generate interatomic force constants $K_{\alpha\beta}$ which can then be employed to investigate the elastic constants

$$K_{\alpha\beta} = \frac{d^2\Phi(r)}{dr_\alpha dr_\beta} = \left[\delta_{\alpha\beta} - \frac{r_\alpha r_\beta}{r^2} \right] K_t + \frac{r_\alpha r_\beta}{r^2} K_\gamma. \quad (8)$$

In the long-wave-phonon approximation, the elastic constants are given by [1–6]

$$C_{11} = \frac{1}{12a} \sum_n N(n) \left[x^2 K_{xx}^n + y^2 K_{yy}^n + z^2 K_{zz}^n \right], \quad (9)$$

$$C_{44} = \frac{1}{24a} \sum_n N(n) \left[(y^2 + z^2) K_{xx}^n + (z^2 + x^2)^2 K_{yy}^n + z^2 K_{zz}^n \right], \quad (10)$$

$$C_{11} + C_{44} = \frac{1}{6a} \sum_n N(n) \left[yz K_{yz}^n + zx K_{zx}^n + xy K_{xy}^n \right], \quad (11)$$

where a is the lattice constant and $N(n)$ is the number of atoms at the n^{th} -neighbour separation.

The shear modulus and bulk modulus are given by [1–5]

$$C' = \left(\frac{C_{11} - C_{12}}{2} \right) \quad (12)$$

and

$$B = \left(\frac{C_{11} + 2C_{12}}{3} \right). \quad (13)$$

The extent to which the interatomic forces are non-pair wise can be obtained by investigating the breakdown of the Cauchy's relation. The Cauchy's ratio is obtained as C_{12}/C_{44} .

The Poisson's ratio is the second independent elastic parameter determined as [1–5],

$$\sigma = \frac{C_{12}}{(C_{11} + C_{12})}. \quad (14)$$

From the calculated values of the bulk modulus and Poisson's ratio, the Young modulus is obtained as [1–5]

$$Y = 3B(1 - 2\sigma). \quad (15)$$

In the cubic system, the propagation velocity of longitudinal and transverse waves in [100], [110] and [111] directions are given as [1–5]

$$v_L[100] = \left[\frac{C_{11}}{\rho} \right]^{1/2}, \quad (16)$$

$$v_L[110] = \left[\frac{C_{11} + C_{12} + 2C_{44}}{2\rho} \right]^{1/2}, \quad (17)$$

$$v_L[111] = \left[\frac{C_{11} + 2C_{12} + 4C_{44}}{3\rho} \right]^{1/2}, \quad (18)$$

$$v_T[100] = v_{T1}[110] = \left[\frac{C_{44}}{\rho} \right]^{1/2}, \quad (19)$$

$$v_{T2}[110] = \left[\frac{C_{11} - C_{12}}{2\rho} \right]^{1/2}, \quad (20)$$

$$v_T[111] = \left[\frac{C_{11} - C_{12} + 2C_{44}}{3\rho} \right]^{1/2} \quad (21)$$

The behaviour of phonon frequencies in the limit independent of direction is given by [1–5]

$$Y_1 = \lim_{q \rightarrow 0} \sum \frac{\omega_i^2(q)}{q^2} = \left[\frac{C_{11} + 2C_{44}}{\rho} \right], \quad (22)$$

and

$$Y_2 = \lim_{q \rightarrow 0} \left(\frac{\omega_{T1}}{\omega_{T2}} \right)^2 = \left[\frac{C_{11} - C_{12}}{2C_{44}} \right]. \quad (23)$$

The degree of elastic anisotropy is the inverse of Y_2 , i.e. [1–5],

$$A = \left[\frac{2C_{44}}{C_{11} - C_{12}} \right]. \quad (24)$$

The value of A is unity when the material is elastically isotropic and differs from unity otherwise.

3. Results and discussion

Instead of taking the concentration average of pure metallic alkali elements, we have treated here $A_{1-x}B_x$ ($A=Na$; $B=Li, K, Rb, Cs$) as a pseudo-alloy-atom (PAA), which is a more meaningful approach [1–5]. Following definitions for the parameters of alloy $A_{1-x}B_x$ is adopted for making the computations of lattice dynamical properties of $Na_{0.5}Li_{0.5}$, $Na_{0.5}K_{0.5}$, $Na_{0.5}Rb_{0.5}$ and $Na_{0.5}Cs_{0.5}$ alloys [1–5],

$$r_C = (1-x)r_{C(A)} + xr_{C(B)}, \quad (25)$$

$$Z = (1-x)Z_{(A)} + xZ_{(B)}, \quad (26)$$

$$\Omega_0 = (1-x)\Omega_{0(A)} + x\Omega_{0(B)}, \quad (27)$$

$$M = (1 - x)M_{(A)} + xM_{(B)}, \quad (28)$$

$$k_F = (1 - x)k_{F(A)} + xk_{F(B)}. \quad (29)$$

The input parameters and constants employed for the present computational study are listed in Table 1. In evaluating integration in Eqs. (4) and (5), the upper limit of integral is taken $40 k_F$ so that, a complete convergence of the model potential is achieved at higher momentum transfer and it covers all the oscillations of the form factor. Therefore, any artificial/fictitious cut-off in the present computations is avoided. We have performed the real space sum analysis up to 33 sets of nearest neighbours in r -space, which are found sufficient for computing the elastic constants and bulk modulus using interatomic force constants, to consider a long-range character for proper convergence of the calculation and to achieve desired accuracy.

TABLE 1. Constants and parameters for equiatomic sodium based binary alloys.

Metal	Z	k_F (au)	Ω_0 (au) ³	r_C (au)
Li	1	0.5890	144.9	0.7736
Na	1	0.4882	254.5	1.2180
K	1	0.3947	481.4	1.4029
Rb	1	0.3693	587.9	1.7877
Cs	1	0.3412	745.5	1.9106

The numerical values obtained for K_γ and K_t are tabulated in Tables 2 and 3. The local-field correlation function of Ichimaru-Utsumi (IU) [11] influences highly the present computation. It is observed from these tables that for higher number of shells, the outcome becomes nearly stabilized and goes towards the convergence of the computations.

In the present computation, the bcc crystal structure is assumed for all binary solid solutions. The lattice constants a are obtained from the well known relation $a = (2\Omega_0)^{1/3}$. Tables 4–7 display the computed values of some lattice dynamical properties of four equiatomic sodium based binary alloys. From Table 3, one can see that our results calculated for C_{11} , C_{12} , C_{44} , $C_{12} - C_{44}$, C_{12}/C_{44} and bulk modulus (B) from H-screening function give the higher values than those for the IU-screening function. A qualitative agreement is found for the calculated values of the shear modulus (C'), deviation from Cauchy's relation, Poisson's ratio (σ), Young modulus (Y), propagation velocities of elastic waves, phonon dispersion curves and degree of anisotropy using H- and IU-screening functions. The experimental values of these properties are estimated for the pure metallic components

TABLE 2. Radial and tangential force constants of equiatomic sodium based binary alloys (in 10^{-3} N/m).

Shell No.	Radial force constants (K_r) for IU-screening				Tangential force constants (K_t) for IU-screening			
	Na _{0.5} Li _{0.5}	Na _{0.5} K _{0.5}	Na _{0.5} Rb _{0.5}	Na _{0.5} Cs _{0.5}	Na _{0.5} Li _{0.5}	Na _{0.5} K _{0.5}	Na _{0.5} Rb _{0.5}	Na _{0.5} Cs _{0.5}
	1	6957.555	4171.407	4448.068	3560.835	-1089.55	-635.789	-714.692
2	2581.365	1537.872	1769.234	1341.708	-346.535	-192.479	-224.454	-163.385
3	157.4532	70.18794	60.07732	49.16526	-20.9041	-12.0548	-14.6056	-11.8247
4	54.73824	38.35456	52.84116	45.24298	-2.68058	-2.18039	-4.1624	-2.70936
5	30.98313	25.72135	43.1961	33.96503	-0.748	-0.71221	-1.92252	-0.89303
6	-6.70049	-5.11975	-3.92997	-7.93248	0.03324	0.335617	0.7897	0.615047
7	-1.37788	-4.10517	-10.3993	-7.94798	-0.36612	-0.15961	-0.04583	-0.24465
8	1.735902	-2.11456	-7.86182	-4.50614	-0.35102	-0.23468	-0.27887	-0.39766
9	3.478589	3.019818	4.79107	6.031671	-0.01441	-0.12254	-0.35391	-0.21035
10	0.784366	2.079436	5.953957	4.194539	0.112532	0.049822	0.014002	0.128149
11	0.784366	2.079436	5.953957	4.194539	0.112532	0.049822	0.014002	0.128149
12	-1.5345	-1.26468	-1.8869	-3.27479	0.015916	0.06966	0.193875	0.123551
13	-0.67625	-1.55582	-3.8411	-3.20843	-0.04149	0.000477	0.045577	-0.03805
14	-0.31628	-1.31334	-3.63047	-2.46322	-0.04823	-0.01891	-0.00777	-0.07747
15	-0.31628	-1.31334	-3.63047	-2.46322	-0.04823	-0.01891	-0.00777	-0.07747
16	0.733582	0.147424	-0.36292	1.251942	-0.02707	-0.04738	-0.12038	-0.1032
17	0.738219	0.823597	1.964008	2.454324	0.004702	-0.02594	-0.08377	-0.02761
18	0.632169	0.884533	2.355235	2.382347	0.012771	-0.01544	-0.05793	0.00053
19	0.020632	0.495261	1.809109	0.534657	0.022917	0.019546	0.043976	0.068859
20	-0.52325	-0.01858	0.1316	-1.06911	0.012689	0.026089	0.072593	0.057405
21	-0.52325	-0.01858	0.1316	-1.06911	0.012689	0.026089	0.072593	0.057405
22	-0.61661	-0.1888	-0.42491	-1.41663	0.008081	0.024319	0.070447	0.044744
23	-0.19324	-0.63506	-1.72664	-1.49713	-0.00814	0.006493	0.023421	-0.01603
24	-0.13313	-0.42268	-1.46366	-0.52931	-0.01222	-0.00798	-0.0204	-0.04286
25	-0.13313	-0.42268	-1.46366	-0.52931	-0.01222	-0.00798	-0.0204	-0.04286
26	0.180892	0.141683	0.259182	1.060882	-0.00518	-0.01522	-0.04557	-0.02718
27	0.320092	0.329757	1.073371	1.221053	0.001303	-0.0094	-0.0285	0.000621
28	0.153423	0.419207	1.211528	1.124402	0.00314	-0.0066	-0.01982	0.009325
29	0.153423	0.419207	1.211528	1.124402	0.00314	-0.0066	-0.01982	0.009325
30	-0.03978	0.358357	1.046366	0.261128	0.006708	0.004583	0.015086	0.029917
31	-0.03978	0.358357	1.046366	0.261128	0.006708	0.004583	0.015086	0.029917
32	-0.06624	0.114324	0.387783	-0.4667	0.005548	0.009399	0.029726	0.026984
33	-0.06624	0.114324	0.387783	-0.4667	0.005548	0.009399	0.029726	0.026984

TABLE 3. Radial and tangential force constants of equiatomic sodium based binary alloys (in 10^{-3} N/m).

Shell No.	Radial force constants (K_r) for IU-screening				Tangential force constants (K_t) for IU-screening			
	Na _{0.5} Li _{0.5}	Na _{0.5} K _{0.5}	Na _{0.5} Rb _{0.5}	Na _{0.5} Cs _{0.5}	Na _{0.5} Li _{0.5}	Na _{0.5} K _{0.5}	Na _{0.5} Rb _{0.5}	Na _{0.5} Cs _{0.5}
	1	5276.62	3362.332	4127.914	3272.414	-501.647	-304.549	-468.444
2	1147.558	758.9882	1317.751	928.5108	-49.9424	-14.295	-63.7379	-28.3685
3	38.81694	-22.253	-109.54	-73.7609	-20.9177	-14.7328	-12.7649	-13.7948
4	96.66559	82.34478	94.23794	96.87666	-3.10645	-4.44188	-9.12709	-6.5544
5	61.88848	64.99227	98.7734	89.12129	0.435952	-1.06083	-4.5346	-2.23234
6	-24.2812	-15.3191	-3.94936	-18.5584	1.332862	1.825485	3.152689	2.798168
7	-12.3736	-18.4098	-35.4249	-31.7908	-0.51139	-0.00042	0.771702	-0.00357
8	-4.26355	-12.9251	-31.1539	-23.3441	-0.70798	-0.40027	-0.10231	-0.70963
9	9.014319	6.980145	7.202149	14.21456	-0.23318	-0.52072	-1.18028	-0.90509
10	4.356379	7.979119	18.16434	15.83236	0.194707	-0.00355	-0.26885	0.12511
11	4.356379	7.979119	18.16434	15.83236	0.194707	-0.00355	-0.26885	0.12511
12	-3.67535	-2.07632	-1.19967	-6.90481	0.116364	0.249077	0.589111	0.481173
13	-2.77218	-4.53279	-10.0791	-10.4337	-0.04727	0.077894	0.280644	0.03686
14	-1.96307	-4.32231	-10.6421	-9.1573	-0.08027	0.015197	0.130403	-0.10183
15	-1.96307	-4.32231	-10.6421	-9.1573	-0.08027	0.015197	0.130403	-0.10183
16	1.201504	-0.80431	-3.814	1.118384	-0.0863	-0.12719	-0.29452	-0.31877
17	1.909999	1.756356	3.590197	6.420076	-0.02015	-0.10135	-0.28231	-0.1584
18	1.803277	2.225931	5.275469	6.889282	0.001693	-0.07687	-0.22792	-0.07991
19	0.447007	2.017328	6.073229	3.233404	0.04933	0.029535	0.056246	0.164542
20	-0.79938	0.565484	2.067003	-1.62404	0.040093	0.068502	0.181715	0.182565
21	-0.79938	0.565484	2.067003	-1.62404	0.040093	0.068502	0.181715	0.182565
22	-1.05923	0.023872	0.47539	-2.92055	0.031712	0.070172	0.192246	0.158628
23	-0.81162	-1.54595	-4.20901	-4.63613	-0.00699	0.035481	0.105754	-0.00221
24	-0.47661	-1.47214	-4.49605	-2.56138	-0.02399	-0.00637	-0.01539	-0.09945
25	-0.47661	-1.47214	-4.49605	-2.56138	-0.02399	-0.00637	-0.01539	-0.09945
26	0.416138	-0.07929	-0.3603	2.303262	-0.01801	-0.04178	-0.12265	-0.09625
27	0.698295	0.702266	2.255915	3.439337	-0.00389	-0.03335	-0.09658	-0.02539
28	0.533018	0.937838	2.834232	3.38112	0.000791	-0.02707	-0.07698	0.000109
29	0.533018	0.937838	2.834232	3.38112	0.000791	-0.02707	-0.07698	0.000109
30	0.170096	1.072646	3.193032	1.470447	0.013272	0.003557	0.017393	0.073631
31	0.170096	1.072646	3.193032	1.470447	0.013272	0.003557	0.017393	0.073631
32	-0.06368	0.600377	1.743836	-0.63785	0.01414	0.020954	0.068714	0.080448
33	-0.06368	0.600377	1.743836	-0.63785	0.01414	0.020954	0.068714	0.080448

[13–17] using PAA model. Qualitative agreement of the present findings due to IU-function is highly encouraging considering the estimated experimental data [13–15] using PAA model. Here, the results due to IU-screening function are much better than those obtained with the help of the static H-screening function. This clearly indicates that the local field correlation plays a very effective role in explaining correctly the static and dynamic properties of such solid solutions. It can be seen from Tables 4–7 that a qualitative agreement is found between estimated experimental values [13–17] using PAA model and present theoretical results when the screening function of IU is used. Also, presently computed results for the lattice dynamical properties of $\text{Na}_{0.5}\text{Li}_{0.5}$, $\text{Na}_{0.5}\text{K}_{0.5}$, $\text{Na}_{0.5}\text{Rb}_{0.5}$ and $\text{Na}_{0.5}\text{Cs}_{0.5}$ binary solid alloys are found in qualitative agreement with the available theoretical data [1] in the literature. The calculated values of C_{11} , C_{12} and C_{44} are not of the desired degree of accuracy because these parameters are computed from the elastic limits of the phonon dispersion curves along three the [100], [110] and [111] directions of high symmetry. It is noticed from the present study that the percentile influence of the IU-local field correction function with respect to the static H-local field correction function on the vibrational properties of $\text{Na}_{0.5}\text{Li}_{0.5}$, $\text{Na}_{0.5}\text{K}_{0.5}$, $\text{Na}_{0.5}\text{Rb}_{0.5}$ and $\text{Na}_{0.5}\text{Cs}_{0.5}$ binary solid alloys is found 2.08%–78.80%, 1.55%–52.89%, 1.02%–35.90% and 2.56%–37.02%, respectively. This clearly indicates that the local field correlations play a very effective role in explaining correctly the static and dynamic properties of such solid solutions. The calculated results of the static and dynamic properties of $\text{Na}_{0.5}\text{Li}_{0.5}$, $\text{Na}_{0.5}\text{K}_{0.5}$, $\text{Na}_{0.5}\text{Rb}_{0.5}$ and $\text{Na}_{0.5}\text{Cs}_{0.5}$ binary solid alloys computed from H- and IU-local field correction functions deviate in the range of 0.64%–180.53%, 0%–173.04%, 0%–212.93% and 1.92%–176.42% from the estimated experimental data [13–17] using the PAA model, respectively.

The H-local field correction function [12] is purely static and it does not include the exchange and correlation effects. The IU-local field correction function [11] is a fitting formula for the dielectric local field correction function of the degenerate electron liquids at metallic and lower densities, which accurately reproduces the Monte-Carlo results and it also satisfies the self consistency condition in the compressibility sum rule and short range correlations. Therefore, the IU-local field correction function affects the longitudinal phonon branches only.

We have also studied the PDC of four equiatomic sodium-based binary alloys viz. $\text{Na}_{0.5}\text{Li}_{0.5}$, $\text{Na}_{0.5}\text{K}_{0.5}$, $\text{Na}_{0.5}\text{Rb}_{0.5}$ and $\text{Na}_{0.5}\text{Cs}_{0.5}$ along the [100], [110] and [111] directions of high symmetry, which are shown in Figures 1–4. We have found that the phonon frequencies in the longitudinal branch are more sensitive to the exchange and correlation effects in comparison with the transverse branches. The frequencies in the longitudinal branch are suppressed due to the IU-screening function than the frequencies due to static H-screening function. But in the transverse branch, the effect of exchange and correlation enhances slightly the phonon modes. It is found that at the zone boundaries of [100] and [111] directions, i.e., for the larger momentum transfer, the effect of local field correlation is almost negligible. These dispersion curves are not showing any abnormality in the three regions of high symmetry directions and exhibit a qualitative behaviour like metallic elements.

TABLE 4. Lattice dynamical properties of $\text{Na}_{0.5}\text{Li}_{0.5}$ alloy.

Properties	H	IU	Expt. [12]	Others [1]
C_{11} in 10^9 N/m ²	25.04	11.44	12.32	11.70, 13, 20.63
C_{12} in 10^9 N/m ²	23.46	10.26	10.03	10.52, 11.63, 19.44
C_{44} in 10^9 N/m ²	7.38	6.73	9.10	6.65, 6.72, 6.74
C' in 10^9 N/m ²	7.89	5.88	9.90	5.90, 5.94, 6.84
B in 10^9 N/m ²	23.98	10.65	11.00	10.92, 12.09, 19.84
$(C_{12} - C_{44})$ in 10^9 N/m ²	16.60	3.52	12.50	3.78, 4.91, 12.78
Cauchy's ratio (C_{11}/C_{44})	3.17	1.52	1.13	1.56, 1.73, 2.92
σ	0.48	0.47	0.45	0.47, 0.47, 0.49
Y in 10^8 N/m ²	2.34	1.73	2.75	1.74, 1.77, 2.01
$v_L[100]$ in 10^3 m/s	5.44	3.68	4.17	3.73, 3.93, 4.95
$v_T[100]$ in 10^3 m/s	2.95	2.82	3.58	2.81, 2.83, 2.83
$v_L[110]$ in 10^3 m/s	6.12	4.56	5.37	4.61, 4.76, 5.63
$v_{T1}[110]$ in 10^3 m/s	2.95	2.82	3.79	2.83, 2.83, 2.91
$v_{T2}[110]$ in 10^3 m/s	0.96	0.83	1.18	0.84, 0.84, 0.90
$v_L[111]$ in 10^3 m/s	6.32	4.82	5.72	4.87, 5.00, 5.85
$v_T[111]$ in 10^3 m/s	1.88	1.76	2.28	1.76, 1.77, 1.79
Y_1 in 10^9 N/m ²	4.71	2.95	4.68	3.00, 3.15, 4.04
Y_2	0.10	0.08	0.11	0.087, 0.089, 0.10
A	9.35	11.45	9.05	9.81, 11.20, 11.42

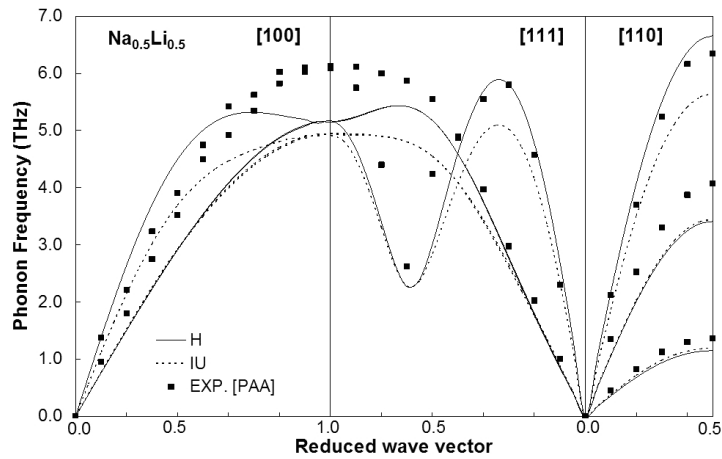


Fig. 1. Phonon dispersion curves of $\text{Na}_{0.5}\text{Li}_{0.5}$ alloy.

TABLE 5. Lattice dynamical properties of $\text{Na}_{0.5}\text{K}_{0.5}$ alloy.

Properties	H	IU	Expt. [12]	Others [1]
C_{11} in 10^9 N/m ²	12.07	8.36	6.54	6.36, 6.67, 10.11
C_{12} in 10^9 N/m ²	11.17	7.26	5.39	5.51, 5.94, 9.40
C_{44} in 10^9 N/m ²	3.55	3.66	4.73	3.18, 3.27, 3.42
C' in 10^9 N/m ²	4.47	5.46	5.75	3.56, 3.67, 4.28
B in 10^9 N/m ²	11.47	7.63	5.78	5.79, 6.18, 9.63
$(C_{12} - C_{44})$ in 10^9 N/m ²	7.62	3.59	8.30	2.09, 2.76, 6.12
Cauchy's ratio (C_{11}/C_{44})	3.14	1.98	1.15	1.61, 1.87, 2.87
σ	0.48	0.46	0.45	0.46, 0.47, 0.48
Y in 10^8 N/m ²	1.32	1.60	1.66	1.05, 1.08, 1.25
$v_L[100]$ in 10^3 m/s	3.56	2.96	2.54	2.59, 2.66, 3.27
$v_T[100]$ in 10^3 m/s	1.93	1.96	2.15	1.83, 1.86, 1.90
$v_L[110]$ in 10^3 m/s	3.99	3.47	3.24	3.14, 3.17, 3.71
$v_{T1}[110]$ in 10^3 m/s	1.93	1.96	2.36	1.83, 1.86, 1.90
$v_{T2}[110]$ in 10^3 m/s	0.68	0.75	0.58	0.61, 0.62, 0.67
$v_L[111]$ in 10^3 m/s	4.12	3.62	3.45	3.31, 3.32, 3.85
$v_T[111]$ in 10^3 m/s	1.24	1.29	1.38	1.17, 1.19, 1.23
Y_1 in 10^9 N/m ²	2.01	1.64	1.62	13.78, 13.96, 17.61
Y_2	0.12	0.14	0.12	0.11, 0.12, 0.13
A	7.94	6.71	8.07	7.99, 8.66, 9.17

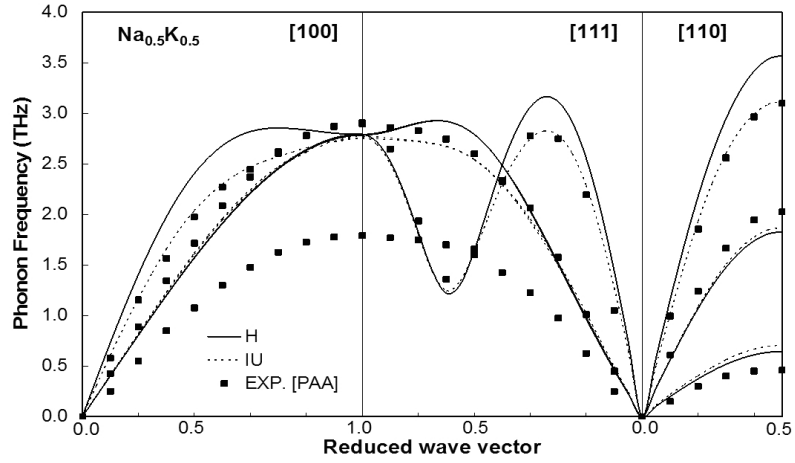


Fig. 2. Phonon dispersion curves of $\text{Na}_{0.5}\text{K}_{0.5}$ alloy.

TABLE 6. Lattice dynamical properties of $\text{Na}_{0.5}\text{Rb}_{0.5}$ alloy.

Properties	H	IU	Expt. [12]	Others [1]
C_{11} in 10^9 N/m ²	12.64	9.57	6.04	4.98, 5.26, 8.00
C_{12} in 10^9 N/m ²	11.64	8.36	4.97	4.30, 4.67, 7.45
C_{44} in 10^9 N/m ²	3.20	2.94	4.35	2.66, 2.73, 2.87
C' in 10^9 N/m ²	4.97	6.04	5.35	2.78, 2.96, 3.43
B in 10^9 N/m ²	11.98	8.76	5.33	4.53, 4.87, 7.63
$(C_{12} - C_{44})$ in 10^9 N/m ²	8.44	5.41	7.40	1.42, 2.01, 4.72
Cauchy's ratio (C_{11}/C_{44})	3.63	2.83	1.16	1.49, 1.76, 2.73
σ	0.47	0.46	0.45	0.46, 0.47, 0.48
Y in 10^8 N/m ²	1.47	1.77	1.55	0.82, 0.87, 1.00
$v_L[100]$ in 10^3 m/s	2.95	2.56	2.17	1.86, 1.91, 2.35
$v_T[100]$ in 10^3 m/s	1.48	1.42	1.83	1.36, 1.38, 1.14
$v_L[110]$ in 10^3 m/s	3.25	2.86	2.27	2.28, 2.30, 2.69
$v_{T1}[110]$ in 10^3 m/s	1.48	1.42	2.35	1.36, 1.38, 1.41
$v_{T2}[110]$ in 10^3 m/s	0.58	0.64	1.00	0.44, 0.45, 0.49
$v_L[111]$ in 10^3 m/s	3.34	2.95	2.23	2.41, 2.41, 2.79
$v_T[111]$ in 10^3 m/s	0.98	0.97	1.73	0.87, 0.87, 0.91
Y_1 in 10^9 N/m ²	1.31	1.06	1.31	7.33, 7.43, 9.33
Y_2	0.15	0.20	0.12	0.10, 0.11, 0.12
A	6.44	4.87	7.83	8.39, 8.98, 9.83

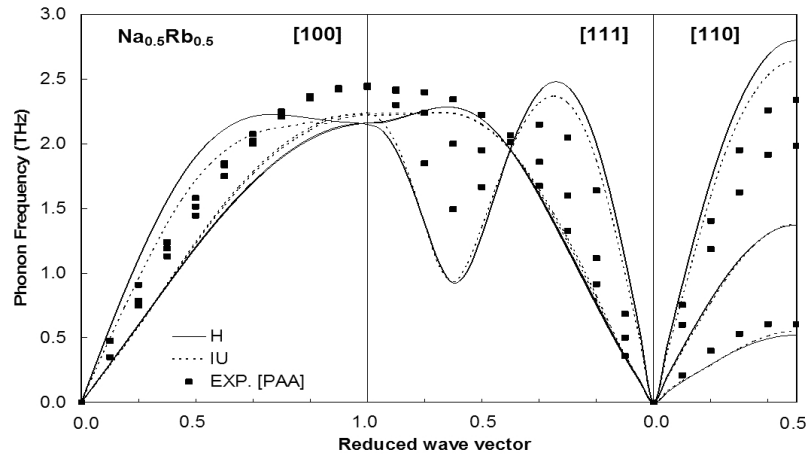


Fig. 3. Phonon dispersion curves of $\text{Na}_{0.5}\text{Rb}_{0.5}$ alloy.

TABLE 7. Lattice dynamical properties of $\text{Na}_{0.5}\text{Cs}_{0.5}$ alloy.

Properties	H	IU	Expt. [12]	Others [1]
C_{11} in 10^9 N/m ²	9.28	6.88	5.76	5.87, 5.95, 8.15
C_{12} in 10^9 N/m ²	8.57	6.02	4.77	5.09, 5.37, 7.53
C_{44} in 10^9 N/m ²	2.51	2.20	4.10	2.30, 2.38, 2.40
C' in 10^9 N/m ²	3.35	4.32	4.95	2.89, 3.08, 3.96
B in 10^9 N/m ²	8.81	6.30	5.10	5.36, 5.56, 7.74
$(C_{12} - C_{44})$ in 10^9 N/m ²	6.05	3.81	6.85	2.72, 3.08, 5.09
Cauchy's ratio (C_{11}/C_{44})	3.40	2.73	1.23	2.14, 2.34, 3.08
σ	0.48	0.46	0.45	0.46, 0.47, 0.48
Y in 10^8 N/m ²	1.05	1.26	1.44	0.85, 0.91, 1.16
$v_L[100]$ in 10^3 m/s	2.30	1.98	2.04	1.84, 1.85, 2.16
$v_T[100]$ in 10^3 m/s	1.20	1.12	1.71	1.15, 1.17, 1.18
$v_L[110]$ in 10^3 m/s	2.55	2.22	2.60	2.12, 2.13, 2.43
$v_{T1}[110]$ in 10^3 m/s	1.20	1.12	1.92	1.15, 1.17, 1.18
$v_{T2}[110]$ in 10^3 m/s	0.45	0.49	0.60	0.41, 0.42, 0.48
$v_L[111]$ in 10^3 m/s	2.63	2.30	2.76	2.21, 2.22, 2.51
$v_T[111]$ in 10^3 m/s	0.78	0.76	1.10	0.74, 0.76, 0.78
Y_1 in 10^9 N/m ²	0.81	0.64	1.22	6.03, 6.09, 7.46
Y_2	0.14	0.19	0.12	0.13, 0.13, 0.17
A	7.08	5.09	7.89	6.00, 7.93, 7.94

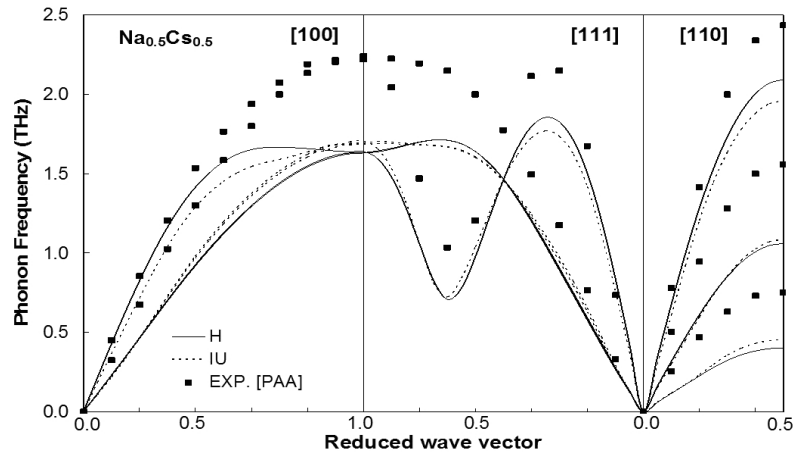


Fig. 4. Phonon dispersion curves of $\text{Na}_{0.5}\text{Cs}_{0.5}$ alloy.

Also, we observed that when we move from $\text{Na}_{0.5}\text{Li}_{0.5}$ to $\text{Na}_{0.5}\text{Rb}_{0.5}$ alloys, the phonon frequency decreases with the increase in the average volume of the solid alloys. As we go from Na to Cs, the atomic volume of the metallic elements is increased. Hence, the average volumes of the solid binary alloys are also increased. The experimental phonon frequencies of such alloys are not available, but the experimental values of phonon frequency are estimated from the pure metallic components [13–17] using PAA model, which are shown in Figs. 1–4. This comparison favours and confirms our formulation of pseudo-alloy-atom (PAA) of the four equiatomic sodium-based binary alloys. Also, in the absence of experimental information, such calculations may be considered as one of the guidelines for further investigations either theoretical or experimental. Hence, such study could be extended for other types of binary alloys.

4. Conclusions

At the end, we conclude that the present form of the pseudo-alloy-atom model (PAA) is successful in explaining the lattice dynamical properties of equiatomic sodium based binary alloys and hence it could be explored for predicting the behavior of other such solid solutions. The comparison of the present theoretical findings with the estimated experimental data helps us to note that the binding of A_{1-x}B_x ($\text{A}=\text{Na}$; $\text{B}=\text{Li, K, Rb, Cs}$) is comparable to the pure metals and hence it behaves like a solid metallic alloy. This can be confirmed by investigating its total crystal energy and heat of solution. Such a study is under progress and the results will be reported in due course of time. From the present experience, we also conclude that it should be interesting to apply other local pseudopotentials for such comprehensive study to judge and confirm the wider applicability of the potential.

References

- [1] A. M. Vora, J. Phys. Chem. Sol. **68** (2007) 1725.
- [2] A. M. Vora, Chinese Phys. Lett. **25** (2008) 654.
- [3] A. M. Vora, Fron. Mater. Sci. China **2** (2008) 315.
- [4] P. N. Gajjar, A. M. Vora, M. H. Patel and A. R. Jani, Different Disordered Systems, eds. Furukawa et al., Indias Publ., Allahabad (India) (2000) 57.
- [5] P. N. Gajjar, B. Y. Thakore, H. K. Patel and A. R. Jani, Acta Phys. Pol. A **88** (1995) 489.
- [6] P. N. Gajjar, B. Y. Thakore, J. S. Luhar and A. R. Jani, Physica B **215** (1995) 293.
- [7] R. F. Wallis, A. A. Maradudin, A. G. Eguluz, A. A. Quong, A. Franchini and G. Santara, Phys. Rev. B **48** (1993) 6043.
- [8] T. Soma, H. Ohsugi and H. Matsuo Kagaya, Phys. State Sol. (b) **124** (1984) 525.
- [9] W. A. Kamitakahara and J. R. D. Copley, Phys. Rev. B **18** (1978) 3772.
- [10] Y. A. Chushak and A. Baumketner, Euro. Phys. J. B **7** (1999) 129.

- [11] N. W. Ashcroft, Phys. Lett. **23** (1966) 48.
- [12] S. Ichimaru, K. Utsumi, Phys. Rev. B **24** (1981) 7385.
- [13] W. Harrison, *Elementary Electronic Structure*, World Scientific, Singapore (1999).
- [14] K. Shimada, Phys. State Sol. (b) **61** (1974) 325.
- [15] H. G. Smith, G. Doling, R. M. Nacklaw, P. R. Vijayraghvan and M. K. Wikinson, *Neutron Inelastic Scattering*, Part I (1968) 149.
- [16] A. D. B. Woods, B. N. Brockhouse, R. H. Marck. A. T. Stewart and R. Bowerson, Phys. Rev. B **128** (1962) 1112.
- [17] R. A. Cowley, A. D. B. Woods and G. Doling, Phys. Rev. B **150** (1966) 487.
- [18] J. R. D. Copley and B. N. Brockhouse, Can. J. Phys. **51** (1973) 657.

DINAMIKA REŠETKE BINARNIH LEGURA SLIČNIH ATOMA

Polazeći od Born von Karmanovih konstanti za središnju silu i zbrajanja u realnom prostoru, proveli smo račune za dinamička svojstva rešetke četiri binarne legure od sličnih atoma, $\text{Na}_{0.5}\text{Li}_{0.5}$, $\text{Na}_{0.5}\text{K}_{0.5}$, $\text{Na}_{0.5}\text{Rb}_{0.5}$ i $\text{Na}_{0.5}\text{Cs}_{0.5}$, do drugog reda u modelnom lokalnom potencijalu. Primijenili smo poznat Ashcroftov potencijal s praznom sredicom za račune dinamičkih svojstava rešetke. Umjesto prosjeka konstanti sila metalnih Li, Na, K, Rb i Cs, pretpostavili smo pseudo-atom legure (PAA) za izravno računanje konstanti sila četiri slično-atomne legure na bazi natrija. Uzeli smo Hartree-eve (H) i Ichimaru-Utsumi-eve (IU) funkcije izmjene i korelacija za istraživanje učinaka zasjenjenja. Ishodi za konstante rešetke, tj. C_{11} , C_{12} , C_{44} , $C_{12} - C_{44}$ i C_{12}/C_{44} , te volumnog modula (B) postignute s Hartree-evom funkcijom zasjenjenja veće su od ishoda tih veličina izračunatih Ichimaru-Utsumi-evom (IU) funkcijom zasjenjenja. Ishodi za modul smika (C'), odstupanje od Cauchy-eve relacije (C_{12}/C_{44}), Poissonov omjer (σ), Youngov modul (Y), brzine elastičnih valova, fononske disperzijske krivulje stupanj anizotropije (A) važni su podaci za ove četiri binarne legure sličnih atoma na bazi natrija.